Supplementary Material for

Revisiting oxo-centered carbonyl-triruthenium clusters: investigating CO photorelease and some spectroscopic and electrochemical correlations

Mariete B. Moreira[a], Camila Fontes Neves da Silva[a], Rafaela B. P. Pesci[b], Victor M. Deflon[b] and Sofia Nikolaou[a*]

[a]Departamento de Química, Faculdade de Filosofia, Ciências e Letras de Ribeirão Preto, Universidade de São Paulo, Av. Bandeirantes 3900, 14040-901, Ribeirão Preto-SP, Brazil, Phone: 55 11 33153748. sofia@ffclrp.usp.br

[b]Instituto de Química de São Carlos, Departamento de Química e Física Molecular – Universidade de São Paulo, Av. do Trabalhador São Carlense 400, Centro ZIP- CODE 13560-970, São Carlos-SP, Brazil.

Table S1. Crystallographic and refinement data for $[Ru_3O(CH_3COO)_6(dmpz)_2(CO)]\cdot H_2O$ (**1**·H_2O), $[Ru_3O(CH_3COO)_6(dmap)_2(CO)]\cdot C_2H_4Cl_2$ (**7**· $C_2H_4Cl_2$), and $[Ru_3O(CH_3COO)_6(4\text{-ampy})_2(CO)]$ (**8**).

Compound	**1**·H_2O	**7**· $C_2H_4Cl_2$	**8**
Empirical formula	$C_{25}H_{36}N_4O_{15}Ru_3$	$C_{29}H_{42}Cl_2N_4O_{14}Ru_3$	$C_{23}H_{30}N_4O_{14}Ru_3$
Formula weight	935.79	1044.77	889.72
Temperature (K)	296(2)	296(2)	296(2)
Wavelength (Å)	0.71073	0.71073	0.71073
Crystal system	Monoclinic	Monoclinic	Orthorhombic
Space group	C2/c	$P2_1/n$	Pnma
Unit cell dimensions	a (Å) = 20.3927(15) b (Å) = 11.1794(8) c (Å) = 17.9721(13) α (°) = 90° β (°) = 119.214(2)° γ (°) = 90°	a (Å) = 13.3193(4) b (Å) = 22.2592(8) c (Å) = 14.4161(5) α (°) = 90º β (°) = 111.062(1)° γ (°) = 90º	a (Å) = 19.2404(4) b (Å) = 19.8237(4) c (Å) = 8.2389(2) α (°) = 90° β (°) = 90° γ (°) = 90°
Z	4	4	4
Density (mg/m^3)	1.738	1.740	1.881
Absorption coefficient (mm^{-1})	1.319	1.321	1.494
F(000)	1864	2088	1760
Crystal size (mm^3)	0.300 x 0.100 x 0.070	0.610 x 0.040 x 0.010	0.140 x 0.060 x 0.030
Theta range for data collection (º)	2.151 to 25.249°	1.769 to 26.404°	2.055 to 25.089°
Index ranges	-23→h→24, -13→k→13, -21→l→21	-16→h→16, -27→k→27, -18→l→ 17	-16→h→22, -20→k→23, -9→l→5
Reflections collected	18964	72486	17509
Independent reflections	3238 [R(int) = 0.0281]	8157 [R(int) = 0.0879]	2884 [R(int) = 0.0393]
Absorption correction	Semi-empirical from equivalentes	Semi-empirical from equivalents	Semi-empirical from equivalents
T_{max}/T_{min}	0.7454/0.6173	0.7454/0.6950	0.7452/0.6797
Data / restraints / parameters	3238 / 0 / 223	8157 / 0 / 479	2221 / 4 / 227
Goodness-of-fit on F^2	1.201	1.020	1.009
Final R indices [I>2σ(I)]	R_1 = 0.0446, wR_2 = 0.0957	R_1 = 0.0428, wR_2 = 0.0952	R_1 = 0.0275, wR_2 = 0.0553
Deposition number*	CCDC 1482393	CCDC 1482394	CCDC 1482395

*Supplementary crystallographic data can be obtained free of charge from The Cambridge Crystallographic Data Centre via www.ccdc.cam.ac.uk/structures.

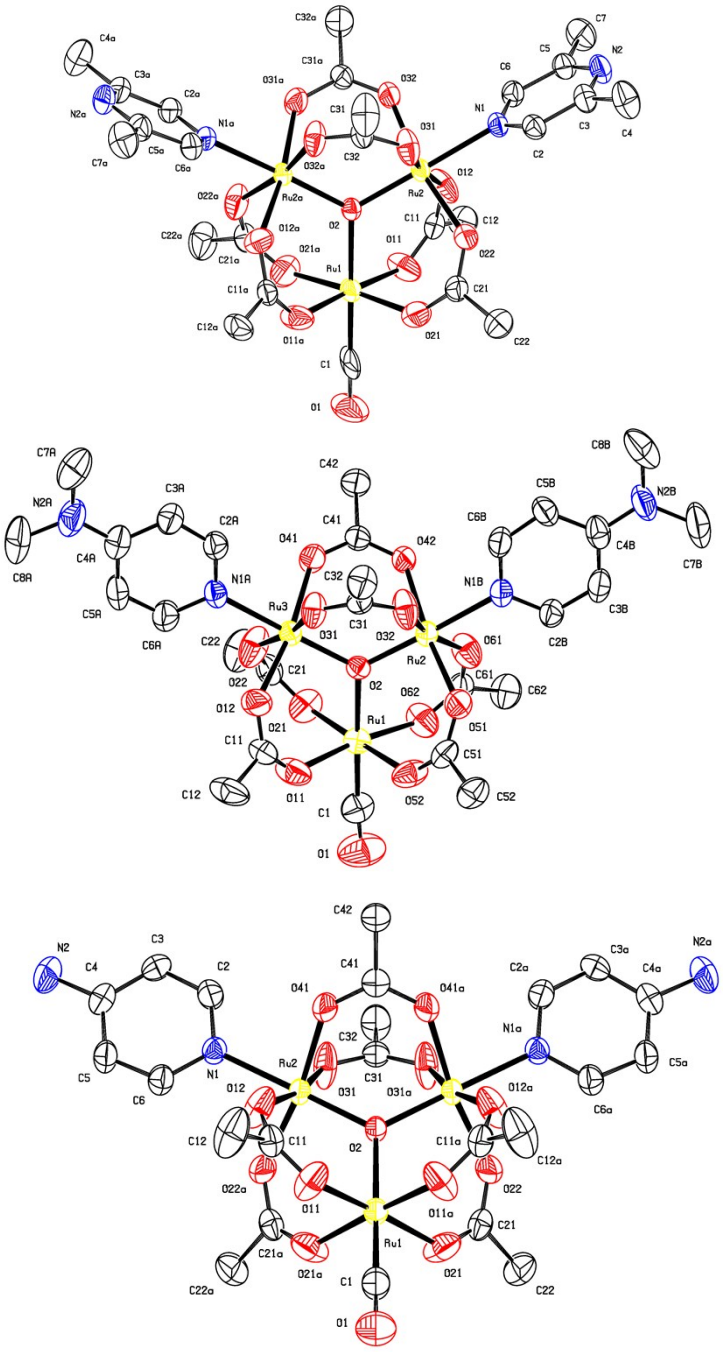

Figure S1. ORTEP plot of complexes $[Ru_3O(CH_3COO)_6CO(L)_2]$ where (top) L = 2,6-dimethylpyrazine (dmpz) (complex **1**), (middle) L = 4-(dimethyl)aminopyridine (dmap) (complex **7**), and (bottom) L = 4-aminopyridine (ampy) (complex **8**)

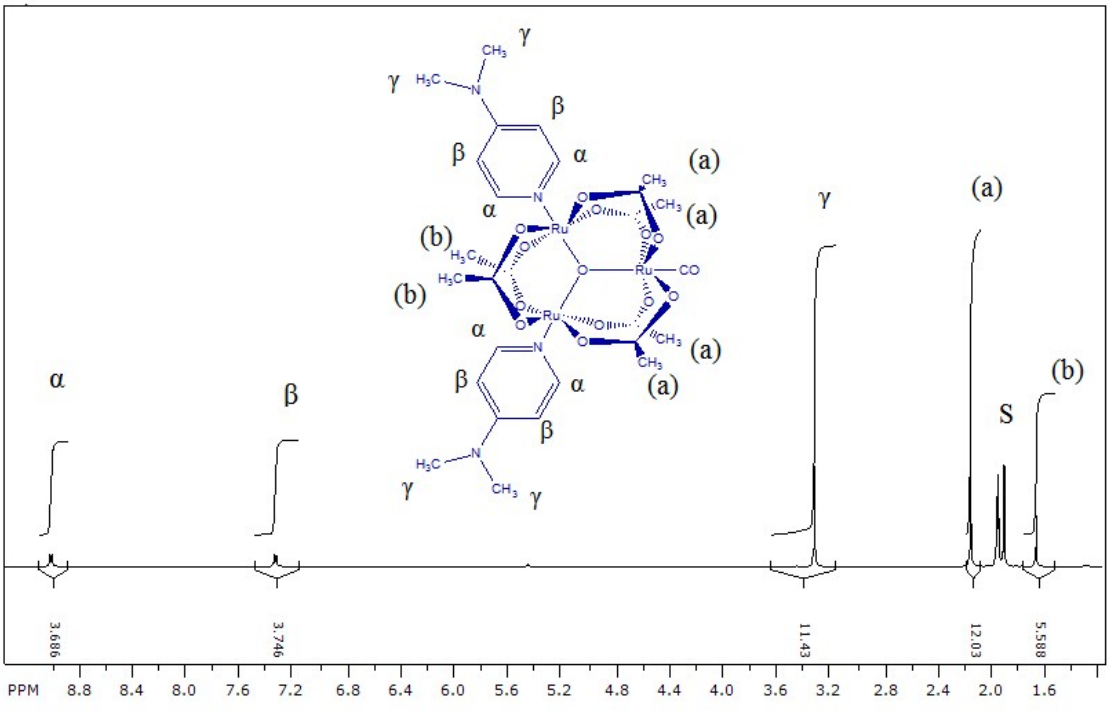

Figure S2. ^{1}H NMR spectrum of the complex $[Ru_3O(CH_3COO)_6(CO)(dmap)_2]$ in CD_3CN at 298 K.

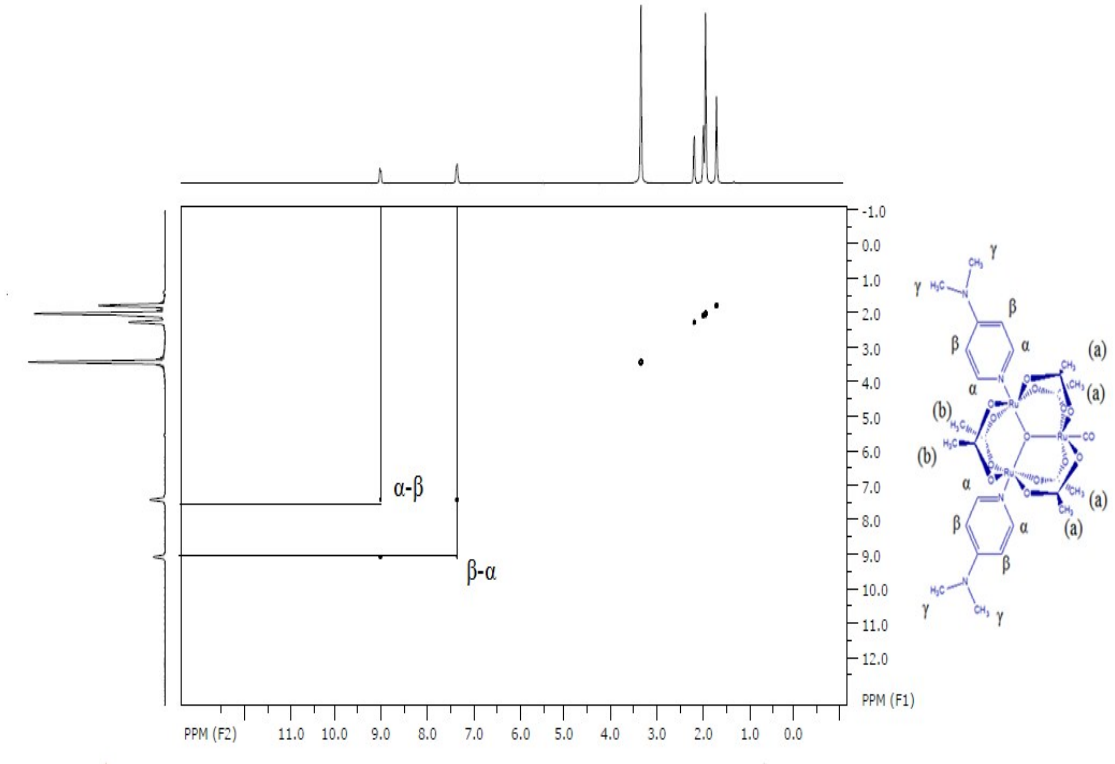

Figure S3. COSY spectrum of the complex $[Ru_3O(CH_3COO)_6(CO)(dmap)_2]$ in CD_3CN at 298 K.

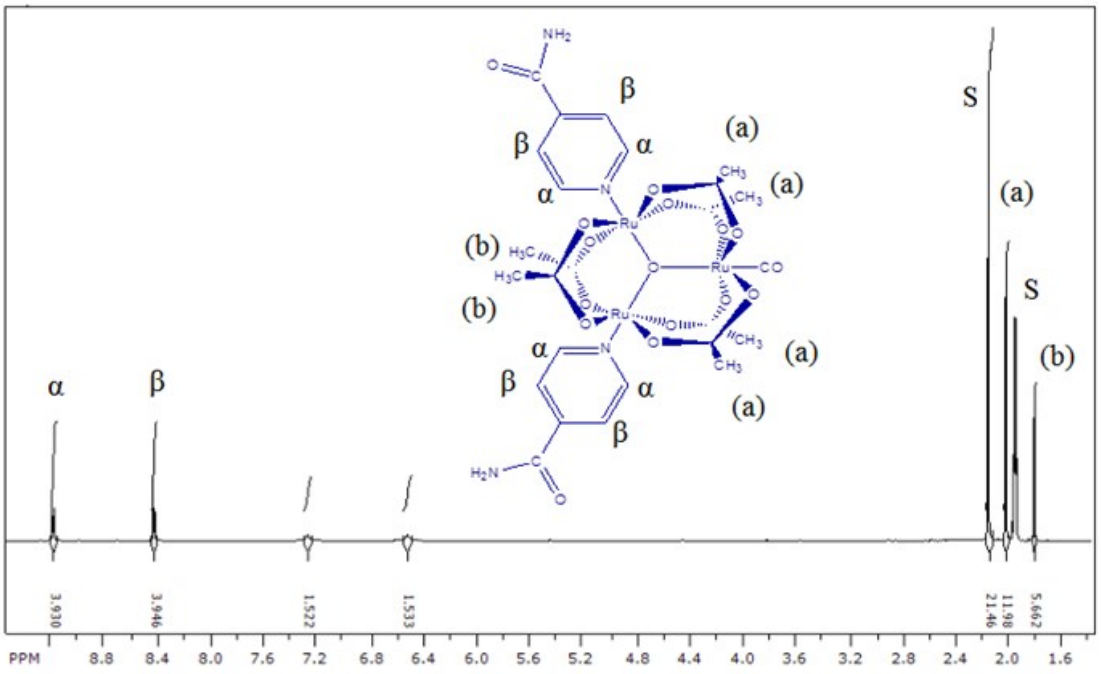

Figure S4. ^{1}H NMR spectrum of the complex $[Ru_3O(CH_3COO)_6(CO)(adpy)_2]$ in CD_3CN at 298 K.

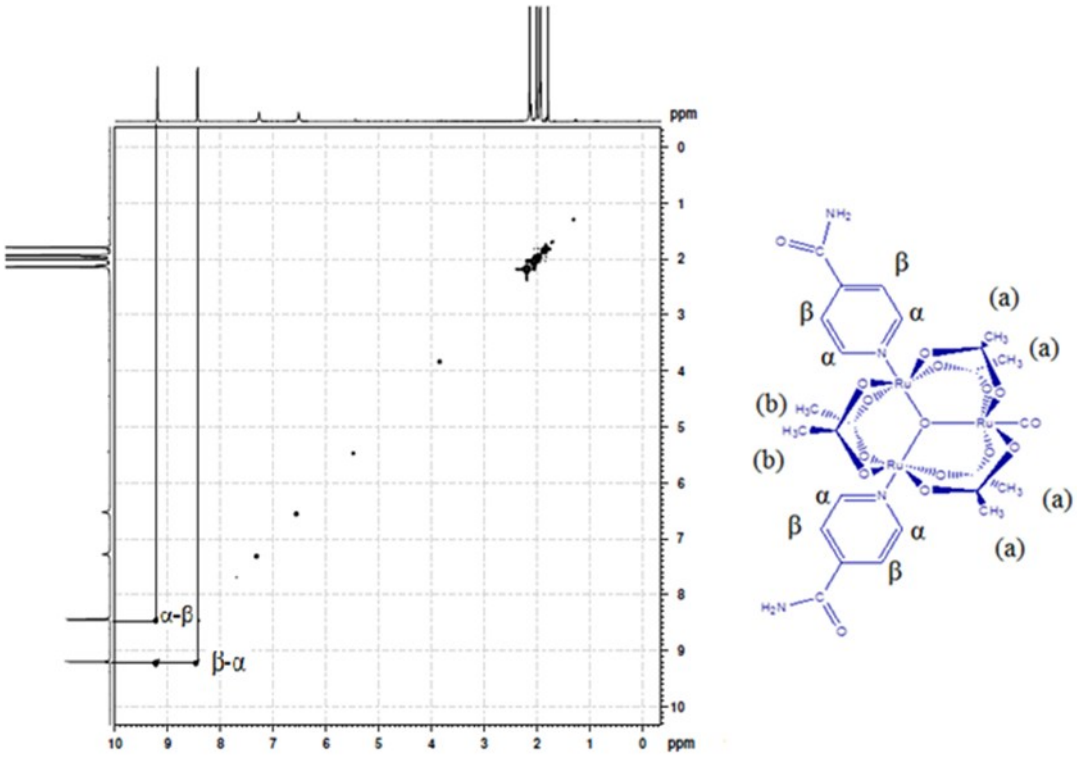

Figure S5. COSY spectrum of the complex $[Ru_3O(CH_3COO)_6(CO)(adpy)_2]$ in CD_3CN at 298 K.

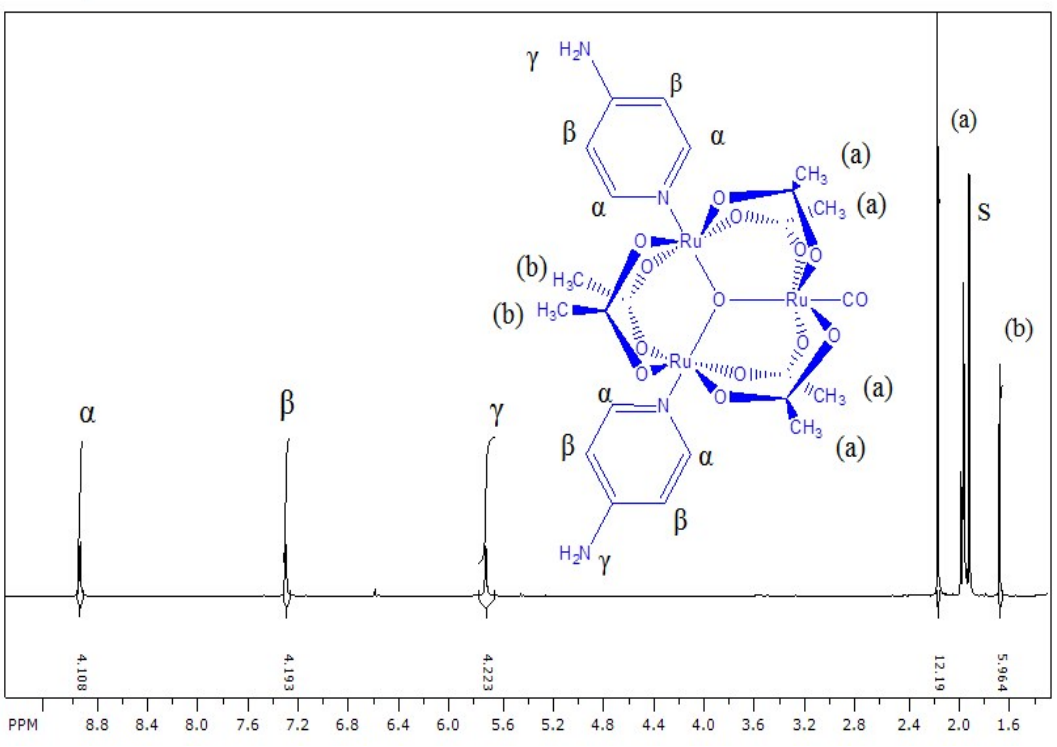

Figure S6. ^{1}H NMR spectrum of the complex $[Ru_3O(CH_3COO)_6(CO)(ampy)_2]$ in CD_3CN at 298 K.

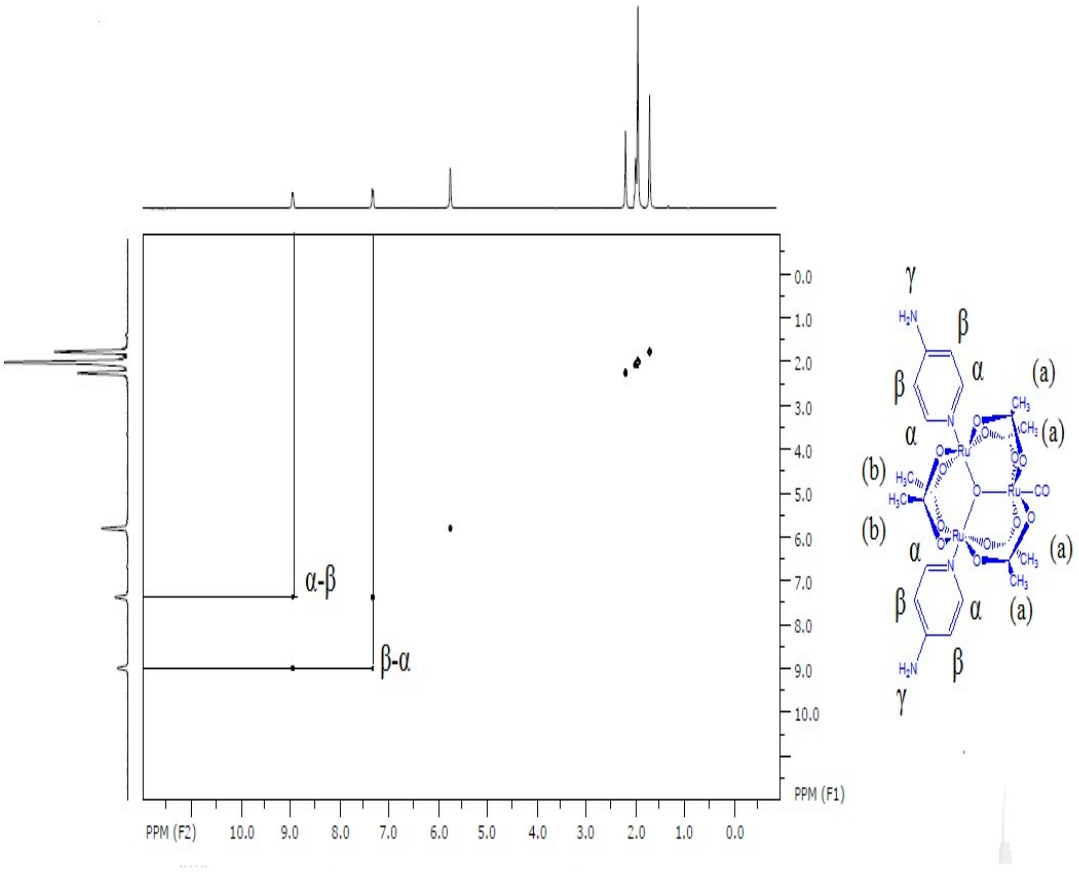

Figure S7. COSY spectrum of the complex $[Ru_3O(CH_3COO)_6(CO)(ampy)_2]$ in CD_3CN at 298 K.

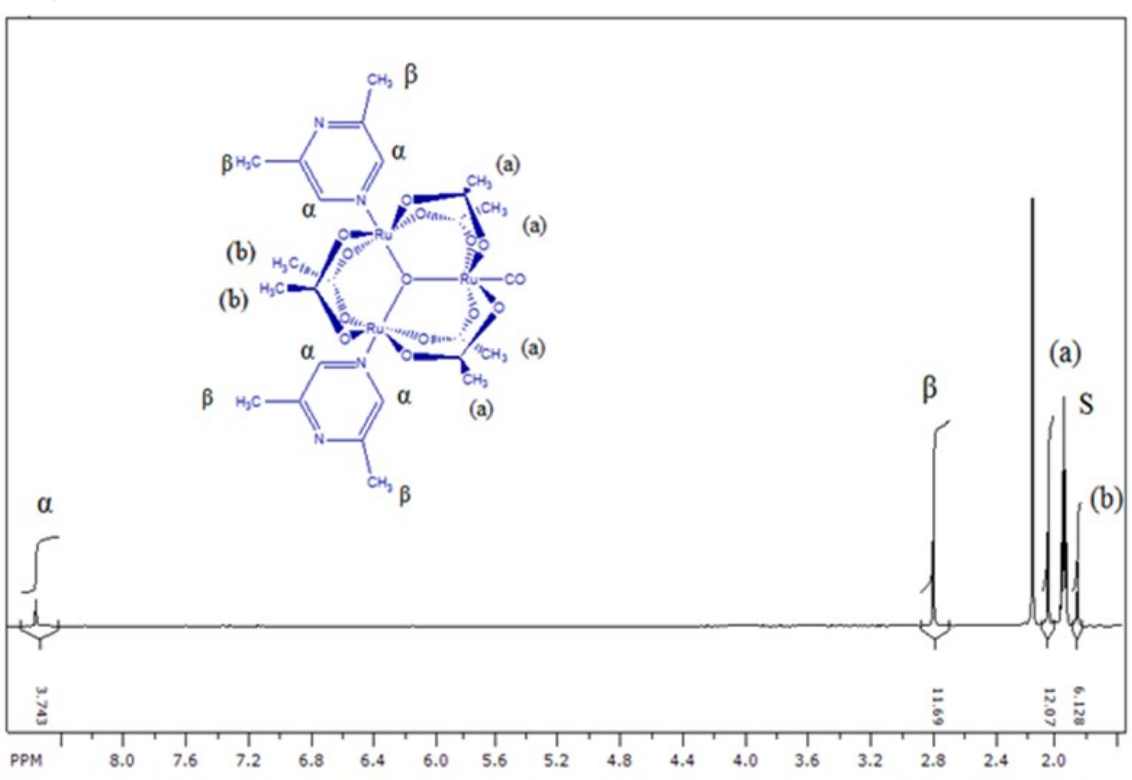

Figure S8. ^{1}H NMR spectrum of the complex $[Ru_3O(CH_3COO)_6(CO)(dmpz)_2]$ in CD_3CN at 298 K.

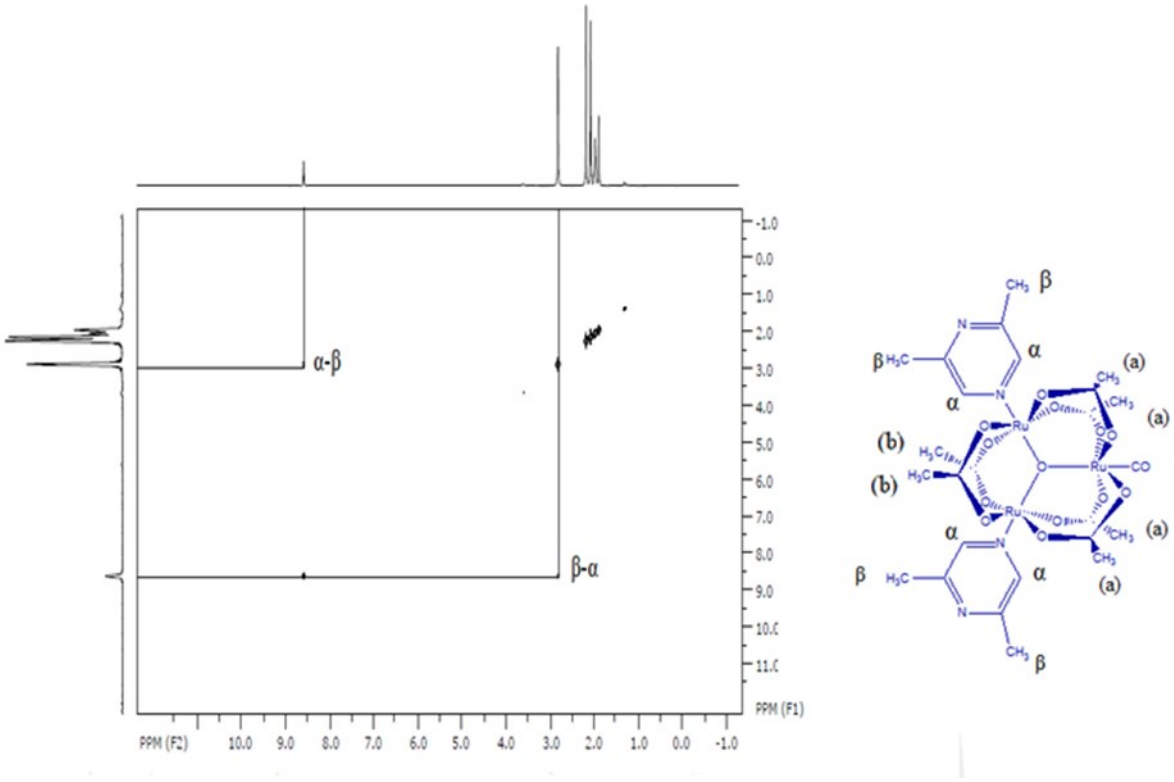

Figure S9. COSY spectrum of the complex $[Ru_3O(CH_3COO)_6(CO)(dmpz)_2]$ in CD_3CN at 298 K.

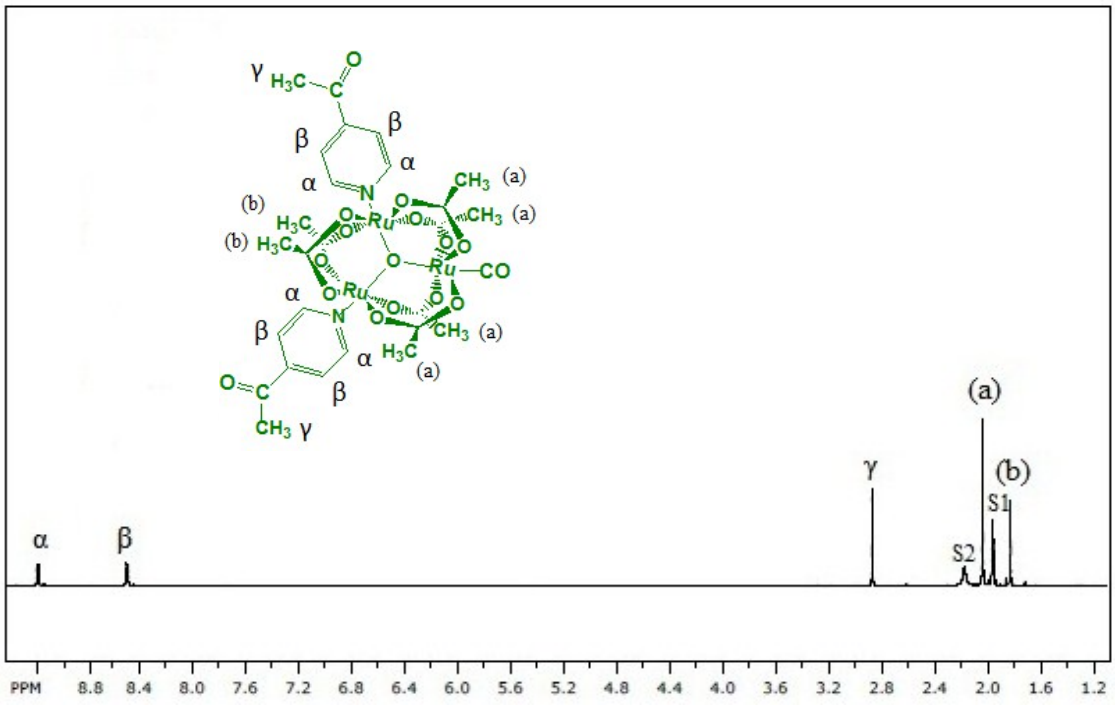

Figure S10. ^{1}H NMR spectrum of the complex $[Ru_3O(CH_3COO)_6(CO)(acpy)_2]$ in CD_3CN at 298 K.

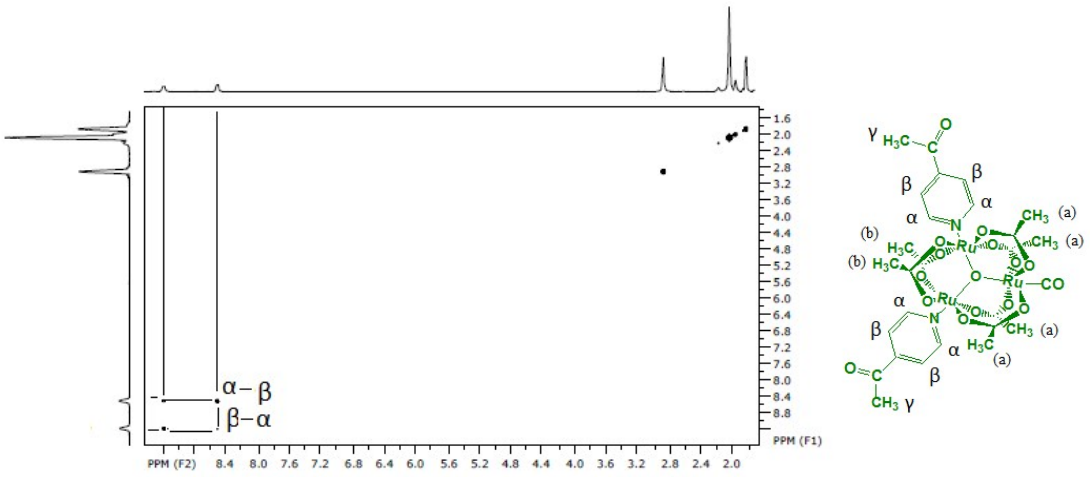

Figure S11. COSY spectrum of the complex $[Ru_3O(CH_3COO)_6(CO)(acpy)_2]$ in CD_3CN at 298 K.

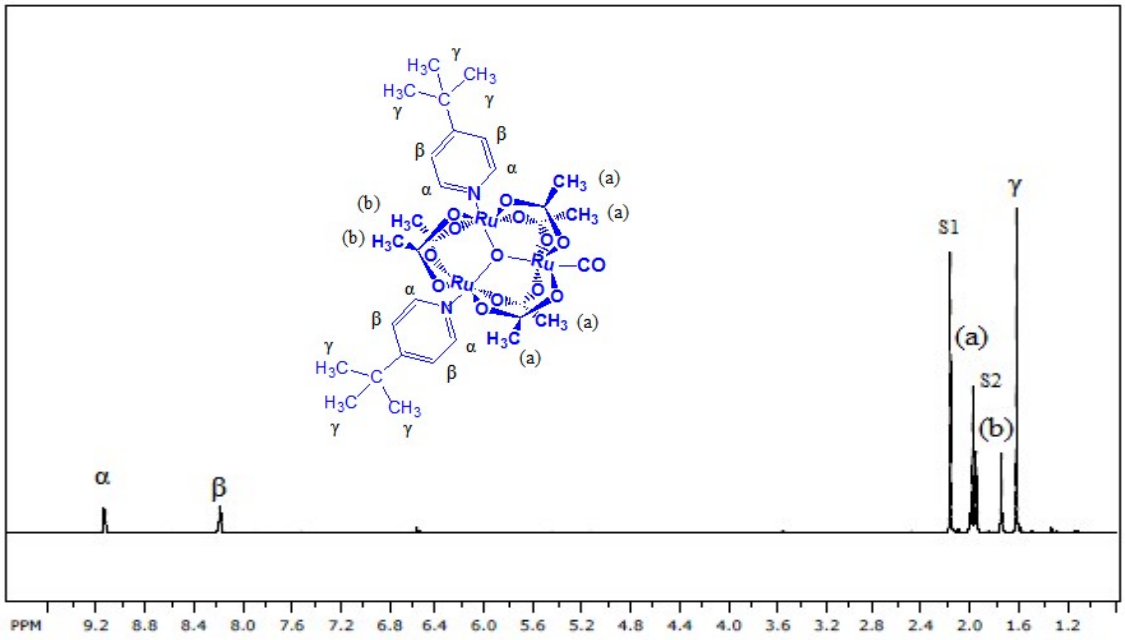

Figure S12. ^{1}H NMR spectrum of the complex $[Ru_3O(CH_3COO)_6(CO)(tbpy)_2]$ in CD_3CN at 298 K.

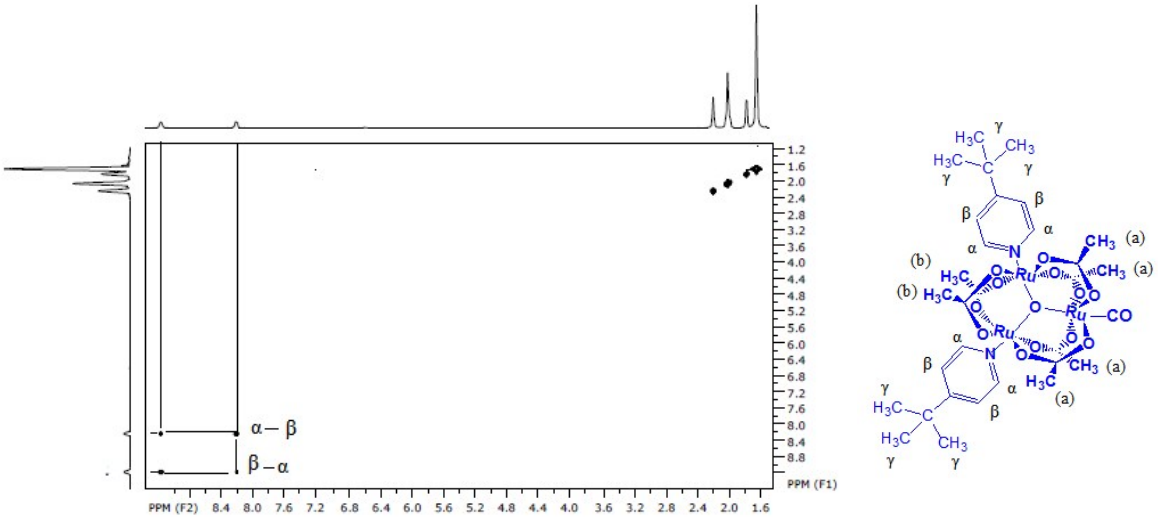

Figure S13. COSY spectrum of the complex $[Ru_3O(CH_3COO)_6(CO)(tbpy)_2]$ in CD_3CN at 298 K.

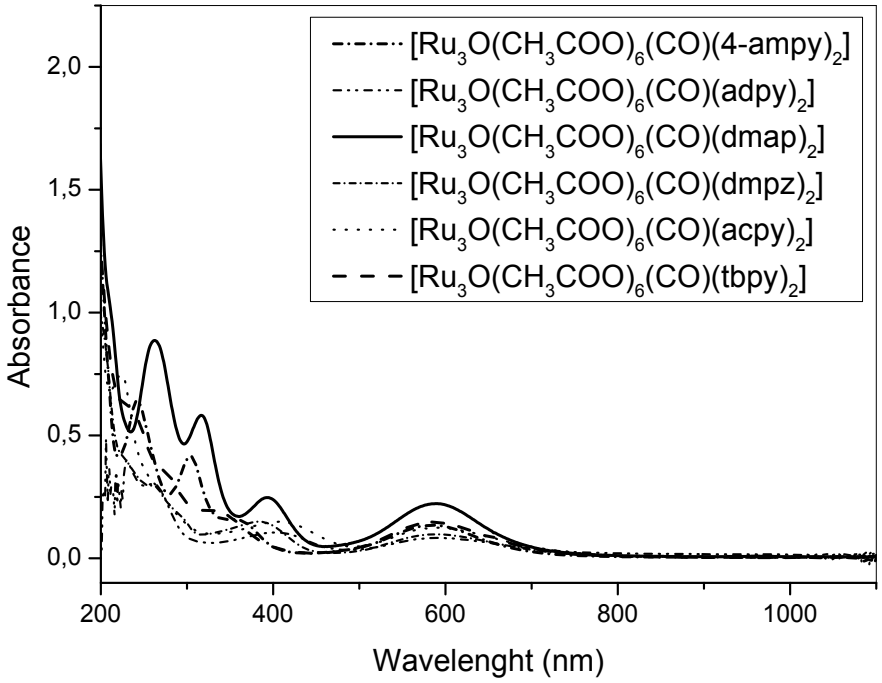

Figure S14. Electronic spectra of compounds of the complexes **1-3** and **6-8** in acetonitrile solutions.

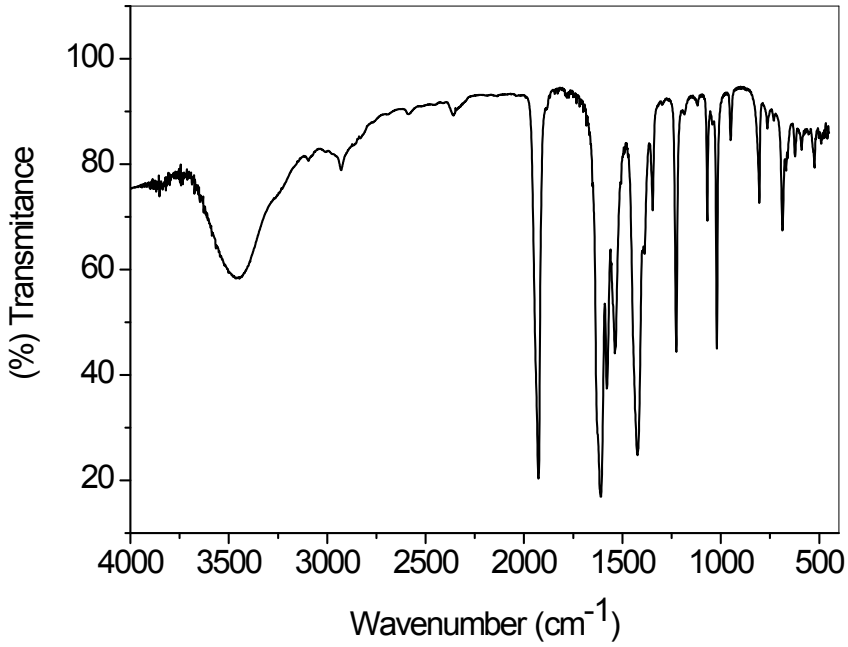

Figure S15. FT-IR spectrum of the complex $[Ru_3O(CH_3COO)_6(CO)(dmap)_2]$, collected from KBr pellets.

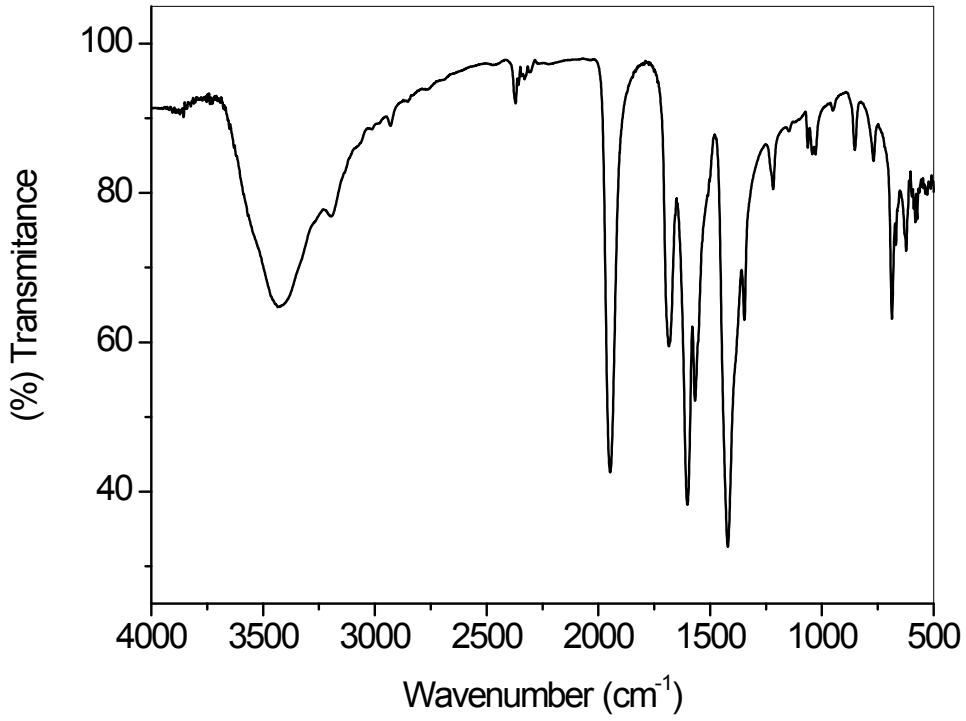

Figure S16. FT-IR spectrum of the complex $[Ru_3O(CH_3COO)_6(CO)(adpy)_2]$, collected from KBr pellets.

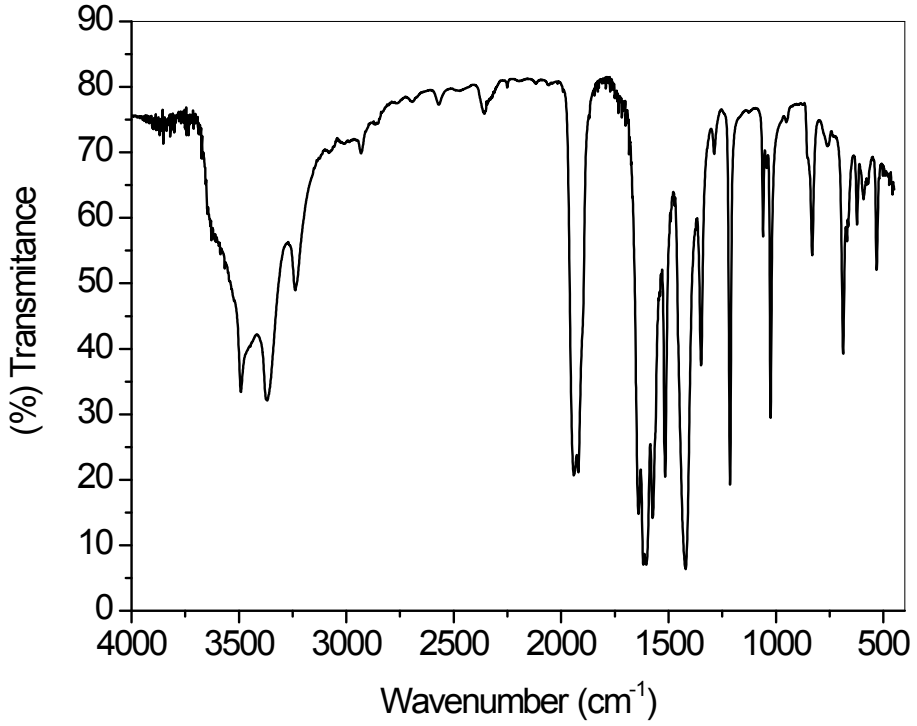

Figure S17. FT-IR spectrum of the complex $[Ru_3O(CH_3COO)_6(CO)(ampy)_2]$, collected from KBr pellets.

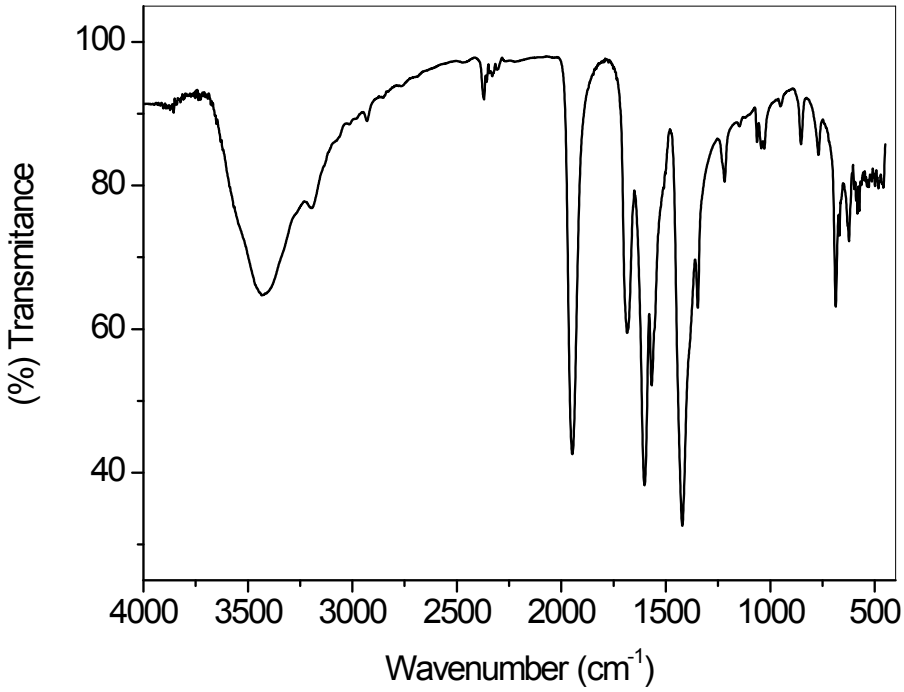

Figure S18. FT-IR spectrum of the complex $[Ru_3O(CH_3COO)_6(CO)(dmpz)_2]$, collected from KBr pellets.

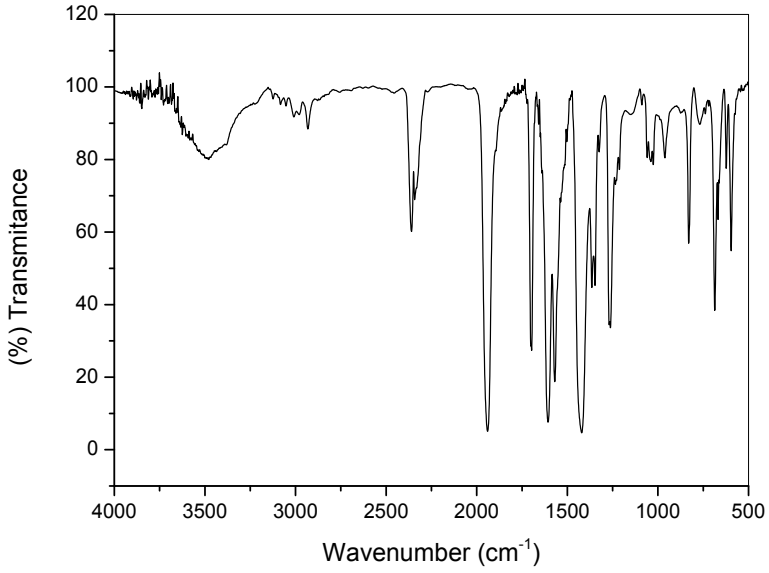

Figure S19. FT-IR spectrum of the complex $[Ru_3O(CH_3COO)_6(CO)(4\text{-acpy})_2]$, collected from KBr pellets.

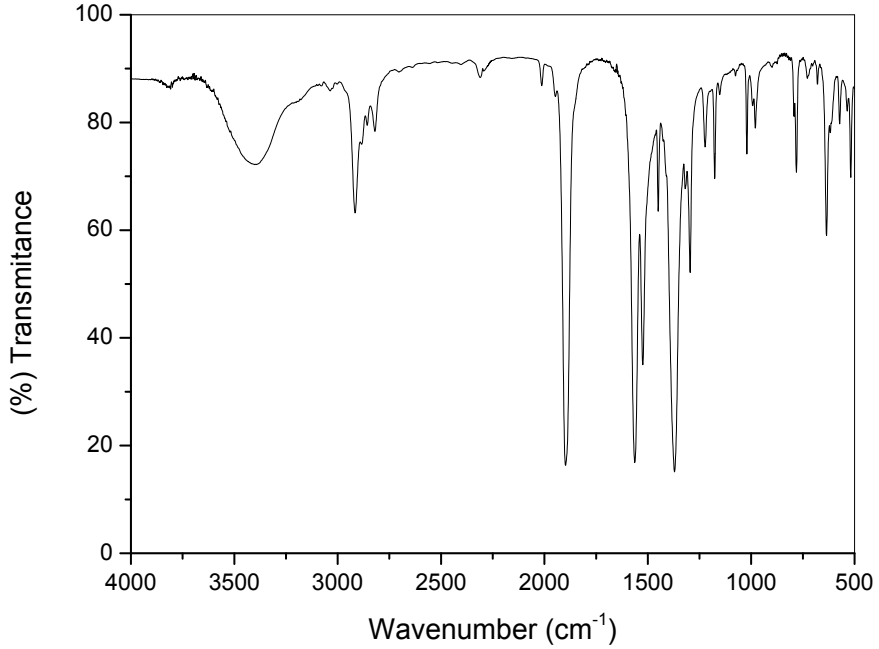

Figure S20. FT-IR spectrum of the complex $[Ru_3O(CH_3COO)_6(CO)(tbpy)_2]$, collected from KBr pellets.

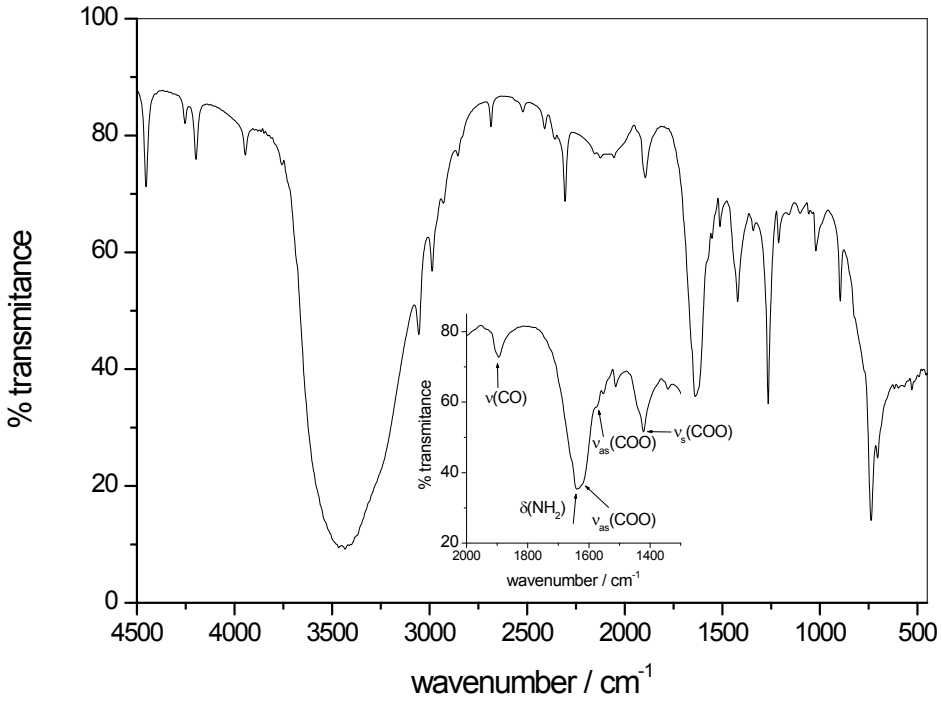

Figure S21. FT-IR spectrum of the complex $[Ru_3O(CH_3COO)_6(CO)(ampy)_2]$, collected in dichloromethane solution, in KBr window (spacer = 0.25 mm).

Table S2: Tentative assignment of the more relevant peaks observed in the infrared spectra, obtained from KBr pellets.

compound	peak (cm^{-1})	assignment
$[Ru_3O(CH_3COO)_6(CO)(adpy)_2]$	1947s	ν(CO)
	1684s	ν(C=O) adpy
	1603s	ν_{as}(COO) Ac
	1566s	ν_{as}(COO) Ac
	1421s	ν_{s}(COO) Ac
	1347w	δ(CH_3) Ac
	1218w	δ(CH) py
	1064w	ν(ring)py
	1029w	δ(CH) Ac
	769w	π(NH) adpy
	687m	δ(OCO)
	624m	π(COO) Ac
$[Ru_3O(CH_3COO)_6(CO)(ampy)_2]$	3377m	ν(NH_2) ampy
	1920s	ν(CO)
	1639s	δ(NH_2) ampy
	1617s	ν_{as}(COO) Ac
	1575s	ν_{as}(COO) Ac
	1420s	ν_{s}(COO) Ac
	1347	δ(CH_3) Ac
	1215m	δ(CH) py
	1060w	ν(ring) py
	1024s	δ(CH) Ac
	687w	δ(OCO)
	622w	π(COO) Ac
$[Ru_3O(CH_3COO)_6(CO)(dmap)_2]$	1927s	ν(CO)
	1611s	ν_{as}(COO) Ac
	1579s	ν_{as}(COO) Ac
	1423s	ν_{s}(COO) Ac
	1346sh	δ(CH_3) Ac
	1227s	δ(CH) py
	1067m	δ(CH) py
	1022s	δ(CH) Ac
	688w	δ(OCO) Ac
	624w	π(COO) Ac
$[Ru_3O(CH_3COO)_6(dmpz)_2(CO)]$	1945s	ν(CO)
	1609s	ν_{as}(COO) Ac
	1569s	ν_{as}(COO) Ac
	1420s	ν_{s}(COO) Ac
	1348w	δ(CH_3)Ac
	1253w	δ(ring in plane) dmpz
	1032w	δ(CH) Ac
	772w	δ(CH) dmpz
	732w	δ(ring) dmpz
	688m	δ(OCO)
	625m	π(COO)Ac
$[Ru_3O(CH_3COO)_6(CO)(4\text{-}acpy)_2(CO)]$	1940s	ν(CO)
	1608s	ν_{as}(COO) Ac
	1569s	ν_{as}(COO) Ac

	1420s	ν_s(COO) Ac
	1347w	δ(CH_3) Ac
	1361w	δ(CH) py
	1058w	ν(ring py)
	1024w	δ(CH) Ac
	683m	δ(OCO)
	623m	π(COO)Ac
	1271s	ν(CH_3) 4-acpy
	1361s	δ_s(CH_3) 4-acpy
	1694s	ν(C=O) 4-acpy
$[Ru_3O(CH_3COO)_6(4\text{-tbpy})_2(CO)]$	1948s	ν(CO)
	1613s	ν_{as}(COO) Ac
	1574s	ν_{as}(COO) Ac
	1421s	ν_s COO) Ac
	1346w	δ(CH_3) Ac
	1273w	δ(CH) py
	1071w	ν(ring) py
	1030w	δ(CH) Ac
	686m	δ(OCO)
	623m	π(COO)Ac
	2963s	δ_s(CH_3) 4-tbpy
	2869s-	ν (CH_3) 4-tbpy

ν = stretching; δ = bending; π: rocking; s = symmetrical; as = assimetrycal; s = strong; m = médium; w = weak; sh = shoulder.

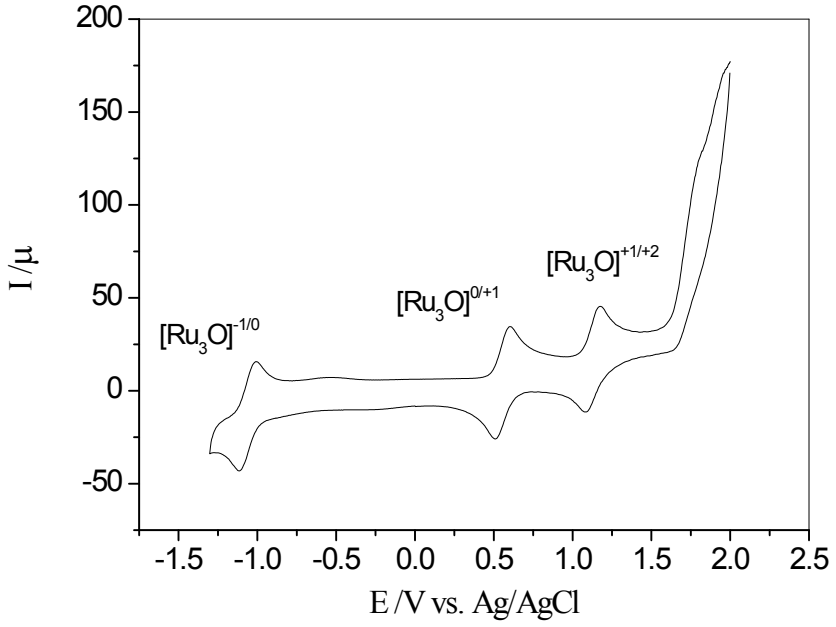

Figure S22. Cyclic voltammogram of compound $[Ru_3O(CH_3COO)_6(CO)(dmap)_2]$ in 0,1 mol dm^{-3} acetonitrile solution $TBAPF_6$. Scan rate 100 mV s^{-1}.

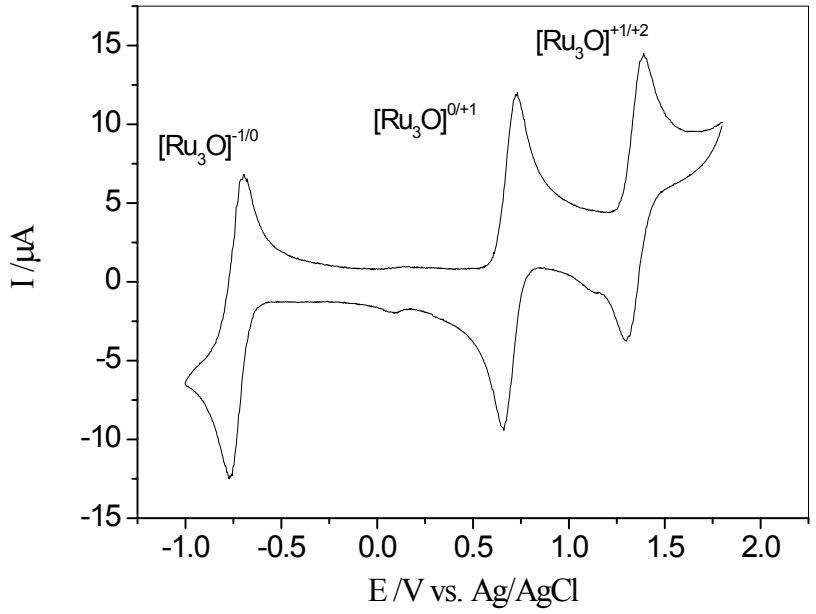

Figure S23. Cyclic voltammogram of compound $[Ru_3O(CH_3COO)_6(CO)(adpy)_2]$ in 0,1 mol dm^{-3} acetonitrile solution $TBAPF_6$. Scan rate 100 mV s^{-1}.

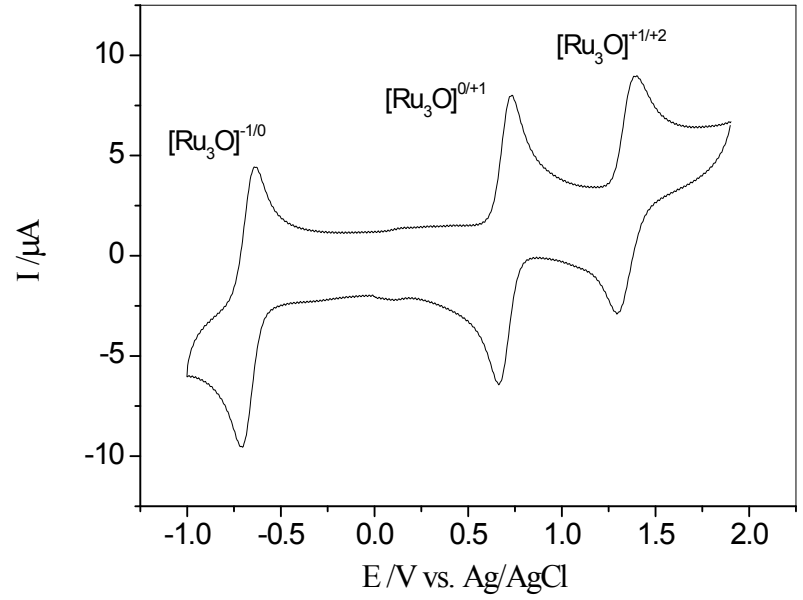

Figure S24. Cyclic voltammogram of compound $[Ru_3O(CH_3COO)_6(CO)(dmpz)_2]$ in 0,1 mol dm^{-3} acetonitrile solution $TBAPF_6$. Scan rate 100 mV s^{-1}.

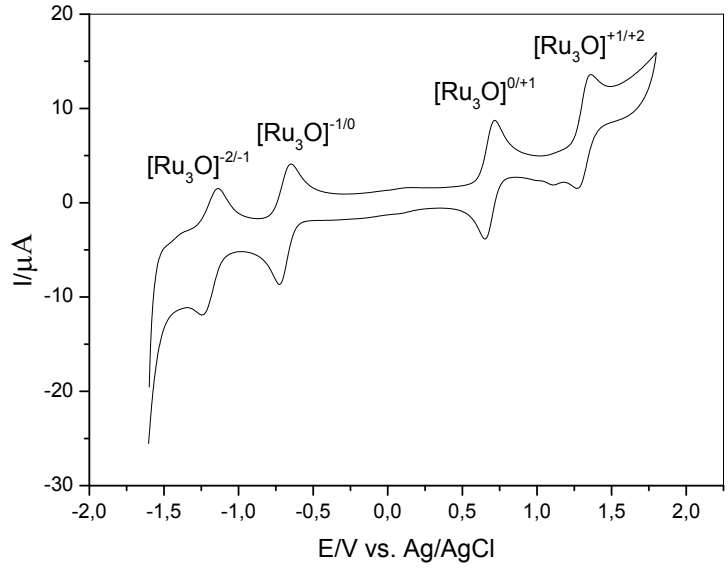

Figure S25. Cyclic voltammogram of compound $[Ru_3O(CH_3COO)_6(CO)(4\text{-acpy})_2]$ in 0,1 mol dm^{-3} acetonitrile solution $TBAPF_6$. Scan rate 100 mV s^{-1}.

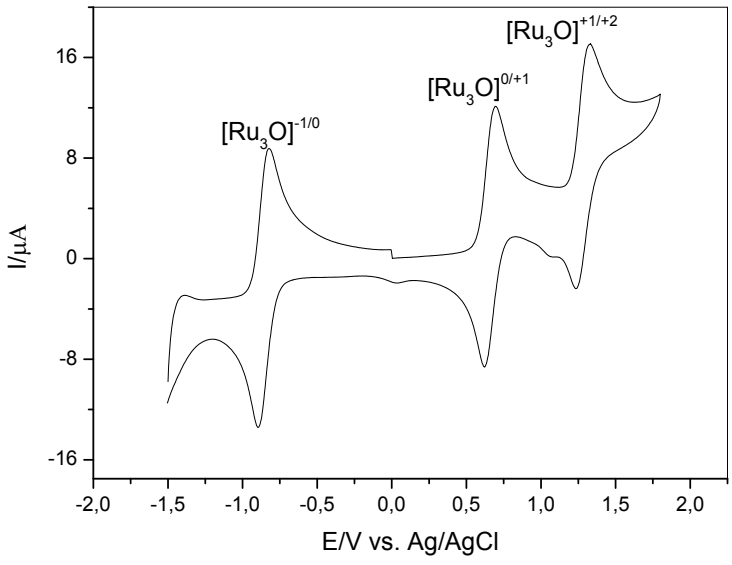

Figure S26. Cyclic voltammogram of compound $[Ru_3O(CH_3COO)_6(CO)(tbpy)_2]$ in 0,1 mol dm^{-3} acetonitrile solution $TBAPF_6$. Scan rate 100 mV s^{-1}.

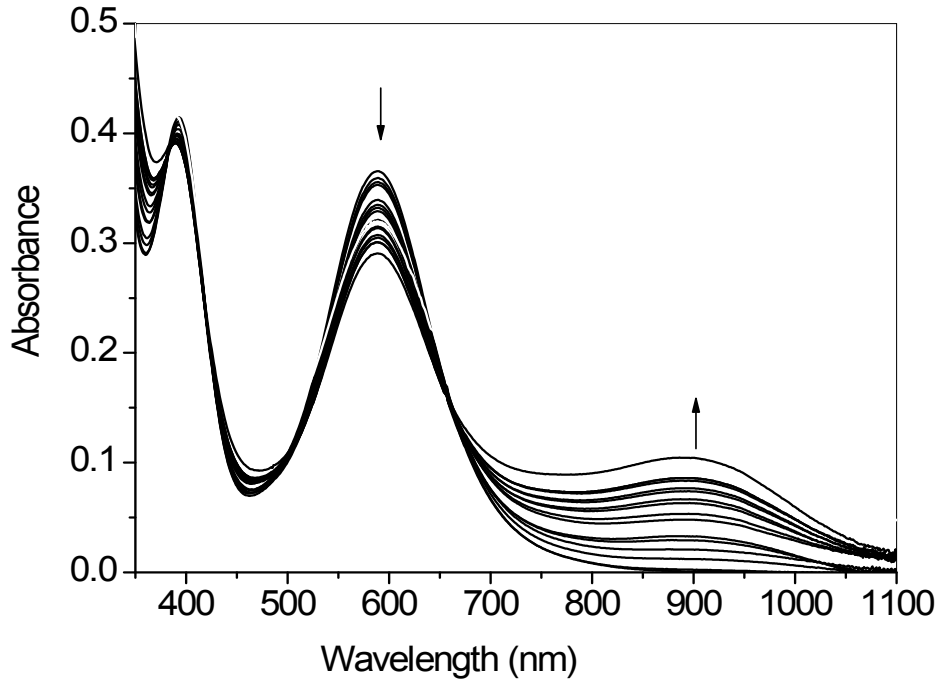

Figure S27. Absorption spectra of complex $[Ru_3O(CH_3COO)_6(CO)(dmap)_2]$ during photolysis at λ_{exc} = 377 nm, collected every 5 minutes from acetonitrile solutions (total time of irradiation = 80 minutes)

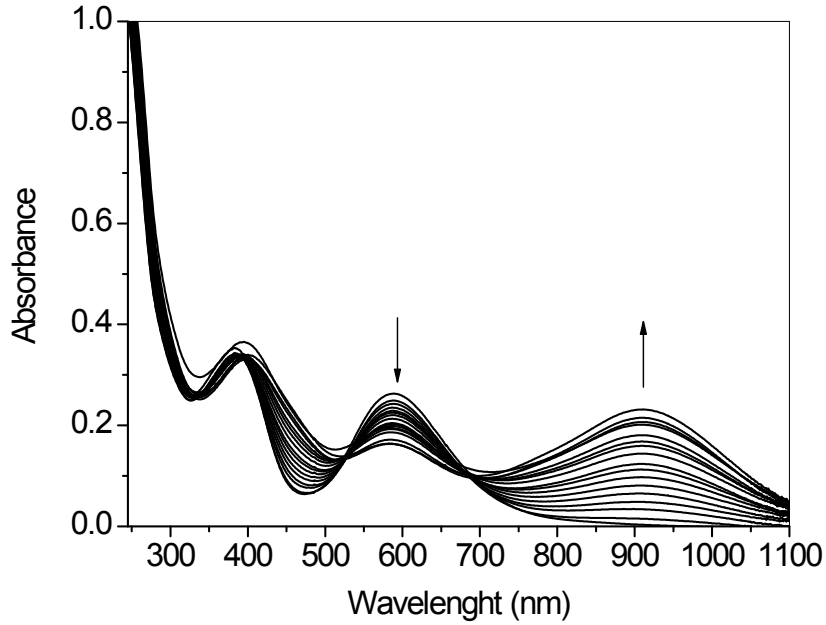

Figure S28. Absorption spectra of complex $[Ru_3O(CH_3COO)_6(CO)(adpy)_2]$during photolysis at λ_{exc} = 377 nm, collected every 5 minutes from acetonitrile solutions (total time of irradiation = 80 minutes)

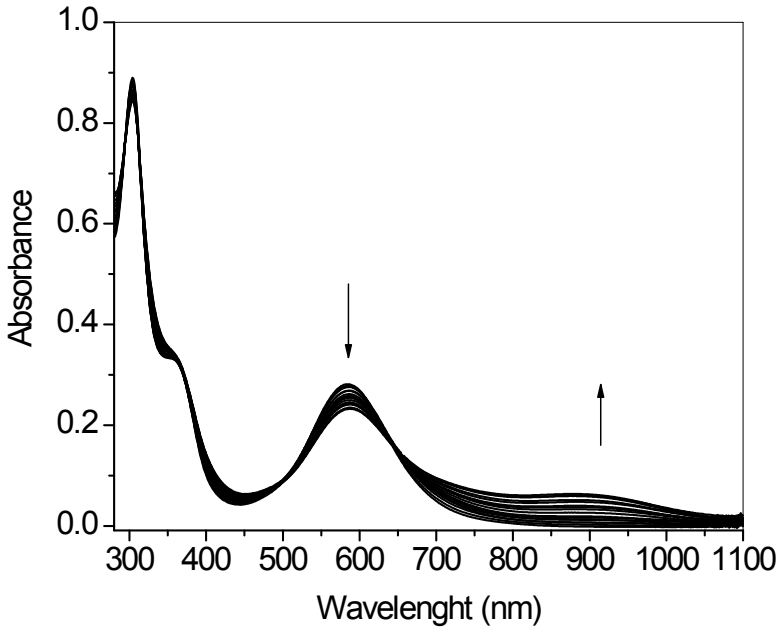

Figure S29. Absorption spectra of complex $[Ru_3O(CH_3COO)_6(CO)(ampy)_2]$ during photolysis at λ_{exc} = 377 nm, collected every 5 minutes from acetonitrile solutions (total time of irradiation = 80 minutes)

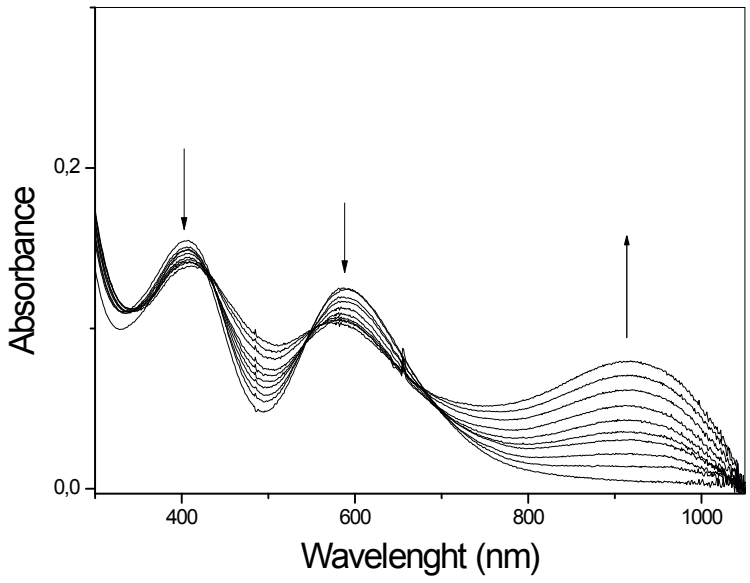

Figure S30. Absorption spectra of complex $[Ru_3O(CH_3COO)_6(CO)(4\text{-acpy})_2]$ during photolysis at λ_{exc} = 377 nm, collected every 5 minutes from acetonitrile solutions (total time of irradiation = 80 minutes)

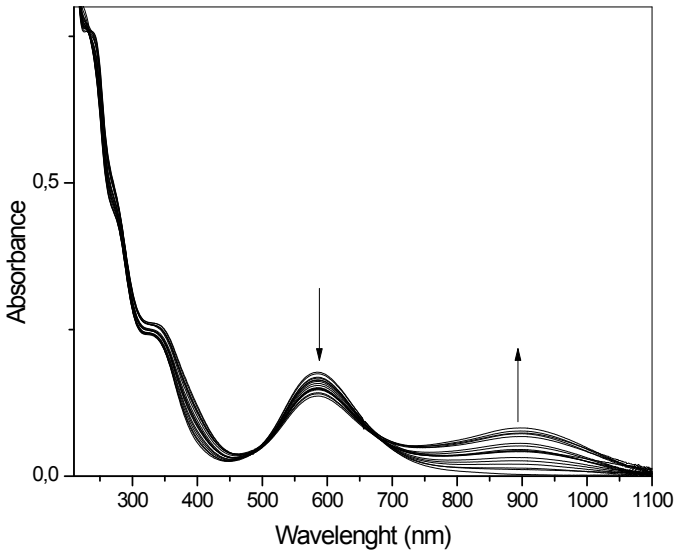

Figure S31. Absorption spectra of complex $[Ru_3O(CH_3COO)_6(CO)(tbpy)_2]$ during photolysis at $\lambda_{exc} = 377$ nm, collected every 5 minutes from acetonitrile solutions (total time of irradiation = 80 minutes)